

Pedestrian Occupancy Prediction for Autonomous Vehicles

Peter Zechel*, Ralph Streiter*, Klaus Bogenberger†, Ulrich Göhner‡

Abstract—This paper presents a new approach to determining the occupancy area of a pedestrian for autonomous driving. To do this, a probabilistic prediction of pedestrian behavior is calculated, which results in the probability of presences. The occupancy prediction can be determined on the basis of this probability as a function of an accepted risk. To predict the behavior, the first step involves using a physical model to determine the possible presence locations. The subsequent assessment of the movement options based on the statistically representative pedestrian behavior, the relevant static objects and the interaction of dynamic objects allows the probabilities of presences to be determined in arbitrary situations. The effectiveness of the prediction is illustrated by using a numerical example which indicates the reduction of occupancy area size by using a suitable prediction method.

Index Terms—occupancy prediction, motion prediction, interaction-aware, autonomous cars

I. INTRODUCTION

Algorithms for autonomous driving consider the occupied area of other traffic participants within a defined prediction time for planing or validating their future maneuvers. Therefore, this occupied area should be on the one hand as small as possible to provide enough drivable space for the autonomous vehicle (AV) but on the other hand large enough to almost certainly include the real object movement. The approach presented in this work tries to fulfill this trade off with a new interaction-aware prediction for pedestrians which focuses on the determination of the occupied area.

To the knowledge of the authors only Koschi [1] presents an approach of determining the occupied area of pedestrians. However, the aim is to include all possible future positions to guarantee the pedestrians safety. In order to realize the trade-off between the size of the occupied area and the prediction safety, the authors believe that including all feasible positions is not suitable, instead the occupied area should be determined by the likely areas of the pedestrian movement. Therefore, the behavior prediction which calculates the probabilistic of presence has to fulfill sophisticated requirements. In the literature a variety of prediction approaches for pedestrians are available. However, applications in this field of work

tend to focus on tracking people [2]–[7] and navigating small robots in an environment full of pedestrians [8]–[12]. Accordingly, the following four requirements, which result from the aim to determine the occupancy prediction, aren't fulfilled by the known approaches, like discussed in the related work section.

- *Differentiated analysis of static objects.* In road traffic, apart from static objects (walls) that cannot be traversed, there are also those objects that influence behavior but can nonetheless be traversed, e.g. sidewalks and lane markers. A suitable prediction method should not categorically rule out the crossing of various static objects, but analyze their influence in a differentiated manner.
- *Interactions between various object classes.* Beside the influence of other pedestrians, the influence of cyclists and vehicles on pedestrians in road traffic is also relevant. The method should therefore consider interactions on a cross-object class basis.
- *Gap-less prediction.* It must be ensured that probable presence locations in the occupancy space are not rejected due to an incomplete prediction.
- *Worst case rather than best fit.* Pedestrians in particular are at risk in road traffic due to their vulnerability; to ensure their integrity the occupancy space should follow a worst-case analysis where doubt exists.

To ensure the method outlined in this paper fulfills the four described requirements, the possible future presence space is analyzed fully in a discrete form in the first step. Using suitable methods each movement option is then assessed on the basis of the following criteria:

- Statistically representative pedestrian behavior, derived from film material from the University of Stanford [13]
- Relevant structural elements of road traffic (e.g. lane markers) and static objects
- Mutual influence of dynamic objects

Finally the assessment of movement options and the future presence locations (FPL) can be combined to determine the probabilities of presence of a pedestrian as a prediction result. To illustrate the prediction part, a numerical example is discussed which finally shows the correct occupancy prediction.

II. RELATED WORK

The following discussion illustrates that, in the authors' view, there is no method familiar from the literature that meets all the requirements set out in this paper, even though

*The authors are with the Daimler AG, RD, Sindelfingen, Germany {peter.p.zechel, ralph.streiter}@daimler.com

†The authors is with the Institute of Traffic Engineering and Regional Planning, Munich University of the Federal Armed Forces, Germany klaus.bogenberger@unibw.de

‡The authors is with the Faculty of Computer Science, University of Applied Sciences Kempten, Germany ulrich.goehner@hs-kempten.de

in some cases impressive prediction results are achieved.

a.) *Approaches with a focus on tracking:* Helbing [2] published in 1998 the first approach considering mutual interaction between pedestrians, called Social Force Model. Luber [3] extends the Social Force Model by including a probabilistic consideration to the prediction. However, Helbing and Luber limit the approach to predicting only one trajectory. Pellegrini [4] presents a model in the shape of Linear Trajectory Avoidance (LTA) which analyzes the interactions with other people not just on the basis of the current position, but extrapolates their behavior. He extends his model in a further publication [6] to include a probabilistic approach. Thus the approach can analyze multiple movement options simultaneously, but due to the computing time requirements places a limit on the analyzed movement options. Besides the usual influences, Yamaguchi [7] models in his approach the coherence of groups and the pull of attractions. In addition, Alahi [5] uses recurrent neural network (RNN) for prediction.

b.) *Approaches with a focus on navigating through crowds:* Helble and Cameron [8] implement a predictive model as part of potential field-based trajectory planning. Using an artificial neural network they, however, predict only one future trajectory. Both the Interaction Gaussian Process Model (IGP) from Trautman [9] and the model from Vemula [10] compute a statistical distribution of the various trajectories, but do not take account of static objects in their prediction. The approaches of Thompson [11] and Bennewitz [12] describe a probabilistic prediction in the indoor area which, in the authors' view, cannot, however, be transferred to the outdoor area. Thompson's [11] requires explicit destinations (desk, printer, etc.) for the prediction, which are difficult to determine for an AV. Bennewitz [12] by contrast uses movement patterns learned from training data to predict the behavior. Given the enormous diversity in road traffic the approach therefore seems unsuitable for an AV.

III. MODEL

The movement of pedestrians is limited by low walking speed and is also highly variable compared with other road users due to rapid changes in direction. Since the required gap-less analysis of the movement options cannot be achieved due to computing time limitations, the authors decided to analyze the movement options discretely through homogeneous discretization of the change in direction and forecast time.

Based on an analysis of the frequencies of various changes in direction in section IV-A it is not productive to analyze angle changes larger than $\psi_{max} = 90^\circ$ due to their low probability of occurrence of 1% compared with the storage and computing resources required. An angular resolution of $\Delta\psi = 5.7^\circ$ (0.1rad) and a temporal resolution $\Delta t = 0.1s$ ensures that the position resolution is always smaller than the size of the pedestrian and still coarsely enough to meet the real time requirements. The chosen prediction time of $t_{max} = 2.5s$ seconds is long enough to respond early on to the movement decisions of pedestrians, while being short enough for the model assumption of a constant angle change

from the start time to be used productively. At this point it must be noted that the parameter ψ_{max} , t_{max} , $\Delta\psi$ and Δt can be changed at any time with quadratic effects on the computing time. Equations 1 and 2 describe the formal discretization of $\Delta\psi$ and Δt , in which ψ_0 describes the current direction.

$$i_{max} = \frac{2 \cdot \psi_{max}}{\Delta\psi} \quad (1)$$

$$\psi(i) = -\psi_{max} + \psi_0 + i \cdot \Delta\psi \quad i \in \mathbb{N} \wedge k \in [0; i_{max}]$$

$$k_{max} = \frac{t_{max}}{\Delta t} \quad t(k) = k \cdot \Delta t \quad k \in \mathbb{N} \wedge k \in [0; k_{max}] \quad (2)$$

To determine the FPLs the change in direction of the pedestrian can be taken into account in various ways. This assumption does not obviously correspond to a natural movement that tends to take place continuously. Nonetheless the model assumption make sense here since it is a worst-case analysis from safety aspects, while also corresponding to the simplest possible theoretical analysis. To take into account the spatial extension, a pedestrian is not analyzed as a point, but as a circle with a defined radius $r_{Ped} = b_{Ped}/2 = 0.3m$. By way of summary the movement modeling is illustrated graphically in Figure 1. In this respect, the rotation can be seen; the center of rotation is not the center of the circle, but in each case on one of the two orthogonal points to the moving direction, called 'corners'. Starting from the current position, the rotation of

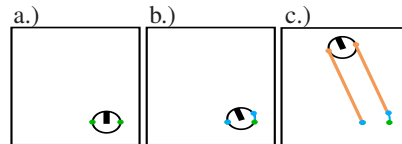


Fig. 1. Pedestrian movement - a.) Starting position $\vec{p}_{L,0}, \vec{p}_{R,0}$ as green points - b.) Position after rotation $\vec{p}_L^R(\psi), \vec{p}_R^R(\psi)$ as blue points - c.) Position after lateral movement $\vec{p}_L^R(\psi, 2.5s), \vec{p}_R^R(\psi, 2.5s)$ as orange points

the pedestrian is taken into account in equations 3 and 4 like illustrated in figure 1. $\mathbf{R}(\psi)$ corresponds to the rotation matrix around the angle ψ , the points $\vec{p}_{R,0}$ and $\vec{p}_{L,0}$ describe the starting positions of the left and right boundary (corner) of the pedestrian vertically to the direction of movement. The result of the equations are the new vertices $\vec{p}_L^R(\psi)$ and $\vec{p}_R^R(\psi)$.

$$\vec{p}_L^R(\psi) = \begin{cases} \vec{p}_{R,0} + \mathbf{R}(\psi) \cdot (\vec{p}_{L,0} - \vec{p}_{R,0}) & \text{if } \psi > 0 \\ \vec{p}_{L,0} & \text{if } \psi < 0 \end{cases} \quad (3)$$

$$\vec{p}_R^R(\psi) = \begin{cases} \vec{p}_{L,0} + \mathbf{R}(\psi) \cdot (\vec{p}_{R,0} - \vec{p}_{L,0}) & \text{if } \psi < 0 \\ \vec{p}_{R,0} & \text{if } \psi > 0 \end{cases} \quad (4)$$

The subsequent calculation in accordance with equations 5 and 6 generates the final trajectories of a pedestrian. The velocity $v = v_0$ is assumed to be constant over the forecast period. The prediction error resulting from this assumption can be regarded as sufficiently small given the prediction

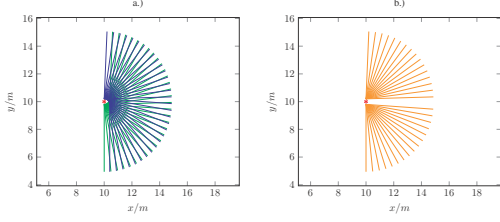


Fig. 2. Calculated FPLs for a pedestrian with $\vec{p}_{L,0} = [10, 10.3]'$, $\vec{p}_{R,0} = [10, 9.7]'$, $\psi_0 = 0^\circ$ and $v_0 = 1 \frac{m}{s^2}$ - a.) $\vec{p}_L^{\rightarrow}(\psi, t)$ in blue and $\vec{p}_R^{\rightarrow}(\psi, t)$ in green - b.) $\vec{p}_T^{\rightarrow}(\psi, t)$ in orange

period of 2.5 seconds.

$$\vec{p}_L^{\rightarrow}(\psi, t) = \vec{p}_L^{\rightarrow}(\psi) + \mathbf{R}(\psi) \cdot (v \cdot t \mathbf{0})' \quad (5)$$

$$\vec{p}_R^{\rightarrow}(\psi, t) = \vec{p}_R^{\rightarrow}(\psi) + \mathbf{R}(\psi) \cdot (v \cdot t \mathbf{0})' \quad (6)$$

The calculated FPLs are shown in figure 2-a. For each analyzed angle a corridor made up of two trajectories is produced; however, many intersect points between the left and right boundary are produced. For the calculation of the probabilities of presence this format is obviously unsuitable since certain locations are reached by multiple movement options. Therefore, a new trajectory array $\vec{p}_T^{\rightarrow}(\psi, t)$ is created per equation 7. This simple resolving of the intersect points is only possible since a suitable rotation center was chosen beforehand, and so the start point is not changed by the rotation for half of the angular range. The final trajectories of the FPLs are shown in graphic 2-b.

$$\vec{p}_T^{\rightarrow}(\psi, t) = \begin{cases} \vec{p}_L^{\rightarrow}(\psi, t) & \text{if } \psi < 0 \\ \vec{p}_R^{\rightarrow}(\psi, t) & \text{if } \psi > 0 \end{cases} \quad (7)$$

IV. ACCEPTANCE DISTRIBUTION

With this approach, the future behavior of a pedestrian identified by index l is determined based on three different influences. Each of these influences is described by its own acceptance distribution; the following sections discuss the modeling, the calculation and the underlying assumptions. The final acceptance distribution, which describes the pedestrian's behavior under all three influences, can be calculated by multiplying the individual acceptance distribution according to equation 8. With this procedure, further influences can be added in the future if so required.

$$f_{l,Akz}(i) = f_{l,Statistic}(i) \cdot f_{l,Static}(i) \cdot f_{l,Dynamic}(i) \quad (8)$$

A. Statistically representative behaviors

This statistical acceptance distribution should map the statistically representative pedestrian behavior. This should result in a prediction as clear as possible when the other influences are subject to a constant acceptance of all movement options, and with untypical behavior first evaluated by a lower acceptance.

To ensure this acceptance distribution has a reliable basis, the typical rotation behavior of pedestrians is determined from the Stanford Drone Dataset [13]. This describes the

pedestrian positions by means of bounding box coordinates. In the first step any pedestrian trajectories are removed from the analysis that do not meet the following requirements:

- Pedestrian trajectory exists for at least $2 \cdot t_{max} = 5s$
- Pedestrians are constantly in motion ($v > 0.65 \frac{m}{s^2}$)
- Bounding box is not too narrow $b_{Boundingbox} > 0.6$

In the simplest case it would be possible to determine the frequency distribution by calculating the angle change between the individual positions as per Figure 3-a. The authors, however, rejected this approach as the dataset provides the position in the form of a bounding box. The information that a pedestrian may be located at any point within this bounding box would be completely ignored by reducing to an individual trajectory. To determine correctly the angle

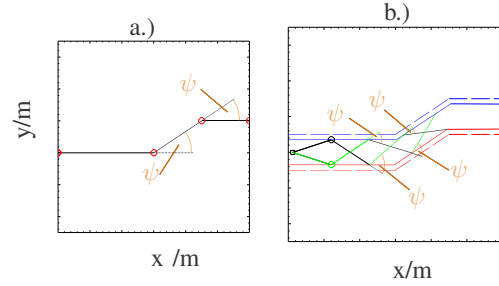


Fig. 3. Example sketch to visualize the determination of the rotation angle - a.) derived trajectory from bounding box - b.) left/right boundary in blue and red, in which dashed lines are the original bounding box width and solid lines are the reduced bounding box width

frequency, the bounding box is converted in the first step to a left/right boundary of the pedestrian movement and this is then narrowed on both sides respectively by a half average pedestrian width ($b_{Ped} = 0.6$). Through this reduction of the possible presence space, the boundaries apply to the center of the analyzed pedestrian.

In the first step of the angle change analysis, a point of the left and right boundary within the distance walked within the forecast period $v \cdot 2.5s$ is determined, starting from the center position at the start time in each case. As a constraint it must be ensured that the connecting line between start point and edge point in each case does not intersect any of the two boundaries. The line between the two determined edge points describes now approximately all possible positions of the pedestrian, who could have reached these positions after 2.5 seconds. Starting from this position description, a point with a distance equal to the distance walked $v \cdot 2.5s$ is now recalculated for the two edge points respectively on the opposite side. With this step the aforementioned constraint must also apply. Through the new edge points another line is determined which describes with the existing line the possible presence locations at two points in time. The analyzed pedestrian could have walked any angle between the extreme values of the two lines to get from line 1 to line 2. Accordingly the frequency in an associated frequency distribution for all angles between the extreme values is in-

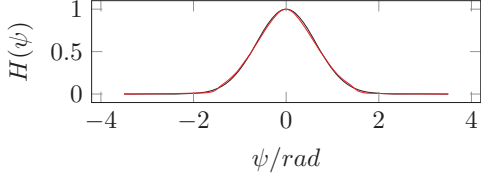


Fig. 4. Result of the frequency analysis in comparison between approximated function in black and relative frequency in red

creased by 1. The process is repeated until the trajectory was analyzed fully. The approach is shown graphically in Figure 3-b. If no points within the distance walked can be found due to the constraint, the required distance is reduced until the constraint is no longer violated to ensure that even these angle changes are registered. The result of the angle change analysis of 20000 trajectories in total with a distance walked of 65 km is illustrated in Figure 4. By approximating the relative frequency distribution the mathematical description in equation 9 was determined with an absolute residual error of 0.1367. Figure 4 shows the approximated function and the relative frequency distribution in comparison.

$$H(\psi) = e^{-1.23758 \cdot \psi^2} \quad (9)$$

The acceptance of a rotation change for the statistical behavior of a pedestrian can be seen as per equation 10 directly from the distribution function.

$$f_{l,Statistic}(i) = e^{-1.23758 \cdot \psi(i)^2} \quad (10)$$

B. Relevant structural elements of road traffic and static objects

This chapter presents the acceptance distribution for quantifying the influence by static objects such as guardrails and curbs as well as structural elements such as lane markers. For this purpose, the static objects must be available in the form of a polygonal line and are indexed using index S .

To quantify the influence, the pedestrian is assumed to avoid static objects proportional to the effort involved in traversing them. Accordingly, a weighting \mathcal{G}^S is added to each polygonal line S that quantifies the effort of traversability in a value range of 0 to 1, e.g. no traversable static objects 1, solid road marking 0.8, dashed road marking 0.1 and curbs 0.1. The weighting of the static objects seems plausible to the authors and demonstrates good results in simulation.

To determine the static acceptance distribution, each polygonal line is intersected with the FPLs of a pedestrian. If there is one or more intersecting points between a polygonal line and future pedestrian positions, the intersecting point with the index of the angle change i and the index of time step k are entered in static collision set $\mathcal{I}_{l,stat} = \{k, i, S | intersect(k, j, S)\}$. The assumption is also made that pedestrians react more intensely to nearby objects than to objects further away. Therefore the period of time of the pedestrian to the possible overrun or collision with an object is taken into account in the assessment. An intersecting point with a polygonal line is thus evaluated using the weighting

and collision time in equation 11. In this equation, the minimum across all evaluated collisions of a considered trajectory i is also formed. The greatest and, thus, most important influence related to a trajectory is therefore factored into the acceptance distribution. Finally, equation 12 is used to calculate the static acceptance distribution $f_{l,Statistic}$. To this end, another minimum operation across all calculated time step is performed to consider the most significant influence (minimum acceptance) per direction.

$$\alpha_{l,stat}(k, i) = \min_{i:(k,i,S) \in \mathcal{I}_{stat}} \left((1 - \mathcal{G}^S) \cdot \frac{t(k)}{t_{max}} \right) \quad (11)$$

$$f_{l,Statistic}(i) = \min_{\forall k} \alpha_{l,stat}(k, i) \quad (12)$$

C. Dynamic objects

The behavior of pedestrians is decisively influenced by other pedestrians as well as by other road users. For quantification of this influence the dynamic acceptance distribution is introduced. The conceptual basis for this is the assumption that pedestrians want to avoid collisions with other objects including other pedestrians. Due to the statistically uneven distribution of probabilities of presence, not all collisions are equally probable. Therefore a initial probability of presence distribution is calculated based on the acceptance distribution from subsections IV-A and IV-B. Although this does neglecter dynamic objects, it does provide an initial estimate of future behavior. To take into account other object types it is assumed that suitable probabilities of presence are also available for these objects. The forced reduction of the acceptance with angle change with a collision risk of zero is not considered practical as pedestrians obviously accept small risks. For instance, the passing of another pedestrian would otherwise not be possible since at all times there is the theoretical risk that a change in direction of the counterpart leads directly to a collision. In view of this consideration, the objective of modeling is to reduce the maximum collision probability for statistically independently moving pedestrians to a minor, accepted risk $P_{col,min}$. For this purpose, a correction factor β_l is determined for each collision from the perspective of each object. This value describes the factor that would be necessary to reduce the resulting collision probability to $P_{col,min}$ when multiplying by one's own probabilities of presence. This is mathematically formulated in equation 13.

$$P_{col,min} = \beta_l(x, y, t) \cdot P_l(x, y, t) \cdot \sum_{l_c: l_c \neq l}^{l_{max}} (\beta_{l_c}(x, y, t) \cdot P_{l_c}(x, y, t)) \quad (13)$$

These correction values serve as a basis for determining the dynamic acceptance distribution. An additional condition must be defined, however, since fully quantifying all correction values by equation 13 is mathematically underdetermined. This is illustrated by the following example: Two pedestrians may have a probability of presence of 90% (pedestrian 1) and 10% (pedestrian 2) at a collision point. To obtain a $P_{col,min}$ of 1% corresponding to equation 13,

any combination of the two correction values β_1 and β_2 can be selected, e.g. $\beta_1 = 1/9, \beta_2 = 1$. However, to ensure that the calculation of β_l is grounded in a reasonable and logical basis, the correction values should be formulated indirectly proportional to the probability of presence. This takes into account the following assumption: Pedestrians who approach a collision point with a low probability tend to avoid the collision as they have other viable alternatives (areas with a high probability) at their disposal. A pedestrian with a high probability at a collision point, however, will be less likely to avoid the collision point due to a lack of alternatives. This additional condition is modeled in equation 14.

$$\frac{\beta_{l_a}(x, y, t)}{\sum_{l_b}^{l_{max}} \beta_{l_b}(x, y, t)} = \frac{P_{l_a}(x, y, t)}{\sum_{l_b}^{l_{max}} P_{l_b}(x, y, t)} \quad (14)$$

From the two fundamental assumptions in formula 13 and 14 equation 15 can be derived, to calculate the individual correction values. Additionally the condition $P_l(x, y, t) \cdot \sum_{l_c: l_c \neq l}^{l_{max}} P_{l_c}(x, y, t) > P_{col, min}$ ensures that only correction factors are calculated if the probability of collision is higher than permitted threshold $P_{col, min}$.

$$\beta_l(x, y, t) = \sqrt{\frac{P_{col, min}}{\sum_{l_c: l_c \neq l}^{l_{max}} [P_{l_c}(x, y, t)]^2}} \quad (15)$$

$\forall P_l(x, y, t) \cdot \sum_{l_c: l_c \neq l}^{l_{max}} P_{l_c}(x, y, t) > 0$

To be able to efficiently determine the correction factors, equation 15 must be discretized. To this end, the FPLs of a pedestrian are intersected with the FPLs of any other object and the calculated collision points stored in the dynamic collision set $\mathcal{I}_{l, dyn} = \{(k, i, P_r) | intersect(k, i, i_r)\}$. Index k describes the time increment of the collision from the pedestrian's perspective, i the change in direction of the pedestrian and P_r the probability of presence of the other object. Using the fully calculated set, it is possible to convert equation 15 to equation 16.

$$\beta_l(k, i) = \sqrt{\frac{P_{col, min}}{\sum_{(k, i): (k, i, P_r) \in \mathcal{I}_{l, dyn}} P_r^2}} \quad (16)$$

In the final step, the dynamic acceptance distribution is determined from the correction factors, because the correction factors determine an individual correction value for each collision on a trajectory. The acceptance distribution, on the other hand, must calculate a resulting correction value that finally evaluates the acceptance of the respective change-in-direction path. A minimum operation across all time steps is performed again to consider the most significant influence (minimum acceptance) per direction.

$$f_{l, Dynamic}(i') = \min_{\forall k} \beta_l(k, i) \quad (17)$$

V. PROBABILITIES OF PRESENCE

This section describes calculating the probabilities of presence. Therefore the probability of a future pedestrian position point $P_l(k, i)$ is simply defined by the value of the predicted direction i in the final acceptance distribution

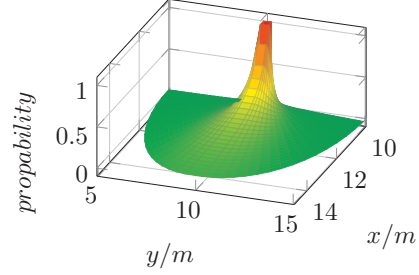


Fig. 5. probability distribution $P_l(k, i)$ based on $f_{l, Akz}(i) = e^{-1.23758 \cdot \psi(i)^2}$ (pedestrian state: $\psi_0 = 0^\circ$, $v_0 = 1 \frac{m}{s^2}$, $x_0 = 10m$ and $y_0 = 10m$)

$f_{l, Akz}$. However, it must be ensured that the sum of all probabilities of a time increment initially correspond with the pedestrian width b_{Ped} . By means of normalization to the pedestrian width b_{Ped} instead of the value 1, the spatial extension is also taken into account in this step. Equation 18 therefore introduces the time-dependent normalization factor c_l and calculates the sum of all probabilities as a double integral via the X and Y positions. In equation 19, the time-dependent normalization factors are used to calculate the probability distribution P_l like discussed before.

$$c_l(k) \cdot \int_x \int_y P_l(x, y) dy dx \stackrel{!}{=} 1 \cdot b_{Ped} \quad (18)$$

$$P_l(k, i) = c_l(k) \cdot f_{l, Akz}(i) \quad (19)$$

The probability distribution $P_l(k, i)$ is the discretized presence probability of the behavior of a pedestrian. The complete prediction of probabilities $P_l(x, y)$ required in the introduction can be made by means of linear approximation based on the four nearest spatial grid points. Points that lie outside the potential future presence areas are assigned a probability of 0.

The prediction result of an example acceptance distribution is shown in Figure 5; the grid structure corresponds to the discretized probability distribution and the area of continuous probability distribution. At the current pedestrian position the probability is 1. Over time the possible presence space of the pedestrian is enlarged whereby the probabilities are increasingly distributed and their amount thus reduced. As a result of the approach described, the prediction rightly becomes more uncertain as the prediction time increases. Finally, it can be ascertained that the projection graphic of the presence probabilities is clearly understandable as results while it can also be transferred very easily to an occupancy area by adding to the occupancy are all presence locations whose probability is greater than a defined risk P_{risk} .

VI. NUMERICAL EXAMPLE

The situation in figure 6 shows a curb which is bordered on the right by a wall and on the left by a road. Two pedestrians move slowly next to each other upwards. A second faster person (blue) is approaching from behind who intends to pass the two slow pedestrians by moving into

the road. This maneuver of the faster considered person can only be predicted by means of a differentiated analysis of static objects in combination with the consideration of object interactions. While fully avoiding static objects, it would not be possible to leave the curb. However, it must be seen in this situation the early hazard detection "Pedestrian might move into the road" is particularly important for AVs to produce an overall safe outcome.

The retention of the current direction along the curb is assessed both by the statistical acceptance distribution and by the static acceptance with the highest value 1 in figure 6-a. The statistical acceptance falls according to the normal distribution with increasing change in direction. By contrast, with the static acceptance the departure toward the road (1.8 to 3.14 rad) via the minimal weighted curb edge is given a relative high acceptance of 0.9. Changes in direction which lead to the wall on the right (0 to 1.1 rad) of the curb receive, by contrast, a small static acceptance value of 0.6. As the curb is blocked by the two slower pedestrians, the dynamic acceptances of all angles, which lead to remaining on the curb (0.6 to 2.2 rad), are sharply reduced. Conversely the remaining angles receive the acceptance value 1. The combination of the three influences produces a significant local maxima at 2.25 rad, which corresponds to a movement toward the road. Combining the acceptance distribution with the possible presence locations shows the correct prediction that the pedestrian intends to move into the road in figure 6-b. Finally the deviated occupied prediction for different P_{risk} is also shown in figure 6-b. The AV will avoid the occupied area for all shown P_{risk} , since the street is always blocked. In addition, the trade off between the size of the occupied area and the safety of the pedestrian is successfully implemented in this example, because even the much smaller black framed area blocks the dangerous part of the street.

VII. CONCLUSION

This paper presents a new method for predicting the behavior of pedestrians. Compared with previous approaches, the focus was particularly on determining the occupancy area for an AV. The advantages lie in a complete probabilistic prediction, a worst-case rather than best-fit modeling, differentiated incorporation of static objects, and suitable consideration of interactions which can process any object class for which a probabilistic prediction model exists. The effectiveness was demonstrated in a numerical example which shows the ability of the approach to reduce the size of occupied area due to the behavior predictions without neglect the dangerous areas.

In future it seems worthwhile to validate the approach in an environment dominated by road traffic. By additionally taking the inaccuracy of sensors into consideration, this approach could be used in a wide range of vehicle assistance systems up to autonomous vehicles.

REFERENCES

[1] M. Koschi, C. Pek, M. Beikirch, and M. Althoff, "Set-Based Prediction of Pedestrians in Urban Environments Considering Formalized Traffic Rules."

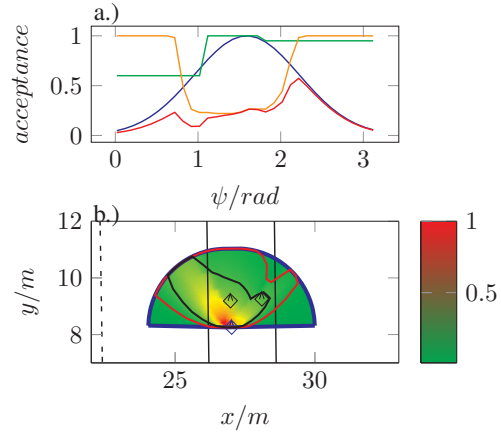


Fig. 6. a.) All acceptance distribution of the evaluated blue vehicle with statistically representative behavior $f_{l,\Pi,Statistic}$ in blue, static objects $f_{l,\Pi,Static}$ in green, dynamic objects $f_{l,\Pi,Dynamic}$ in orange and final acceptance distribution $f_{l,Akz}$ in red - b.) Situation including lane markings, not evaluated pedestrians in black, the probability of presence P_l and occupied areas framed in blue $P_{risk} = 0$, in red $P_{risk} = 0.05$, in black $P_{risk} = 0.1$ of the evaluated blue pedestrian - Measured calculation time in MatrixX is 0.3s expected time in C++ is 3ms based on a single core 3.5 GHz desktop CPU

[2] D. Helbing and P. Molnar, "Social force model for pedestrian dynamics," *Phys. Rev. E*, vol. 51, no. 5, pp. 4282–4286, 1995.

[3] M. Luber, J. A. Stork, and K. O. Arras, "People tracking with human motion predictions from social forces," in *IEEE International Conference on Robotics and Automation*, 2010, pp. 464–469.

[4] S. Pellegrini, A. Ess, K. Schindler, and L. V. Gool, "You'll never walk alone: Modeling social behavior for multi-target tracking," in *12th International Conference on Computer Vision*, 2009, pp. 261–268.

[5] A. Alahi, K. Goel, V. Ramanathan, A. Robicquet, L. Fei-fei, and S. Savarese, "Social LSTM : Human Trajectory Prediction in Crowded Spaces," in *IEEE Conference on Computer Vision and Pattern Recognition*, 2016, pp. 961–971.

[6] S. Pellegrini, A. Ess, and M. Tanaskovic, "Wrong Turn – No Dead End : a Stochastic Pedestrian Motion Model," in *IEEE Computer Society Conference on Computer Vision and Pattern Recognition - Workshops*, 2010, pp. 15–22.

[7] K. Yamaguchi, A. C. Berg, L. E. Ortiz, and T. L. Berg, "Who are you with and Where are you going ?" in *CVPR 2011*, 2011.

[8] H. Helble and S. Cameron, "3-D Path Planning and Target Trajectory Prediction for the Oxford Aerial Tracking System," in *2007 IEEE International Conference on Robotics and Automation*, no. April, 2007, pp. 10–14.

[9] P. Trautman and A. Krause, "Unfreezing the Robot : Navigation in Dense , Interacting Crowds," in *IEEE/RSJ International Conference on Intelligent Robots and Systems*, 2010, pp. 797–803.

[10] A. Vemula, K. Muelling, and J. Oh, "Modeling Cooperative Navigation in Dense Human Crowds," in *IEEE International Conference on Robotics and Automation (ICRA)*, 2017, pp. 1685–1692.

[11] S. Thompson, T. Horiuchi, and S. Kagami, "A Probabilistic Model of Human Motion and Navigation Intent for Mobile Robot Path Planning," in *4th International Conference on Autonomous Robots and Agents*, 2009, pp. 663–668.

[12] M. Bennewitz, W. Burgard, G. Cielniak, and S. Thrun, "Learning Motion Patterns of People for Compliant Robot Motion," *The International Journal of Robotics Research*, vol. 24, no. 1, pp. 31 – 48, 2005.

[13] A. Robicquet, A. Sadeghian, A. Alahi, and S. Savarese, "Learning Social Etiquette : Human Trajectory Understanding in Crowded Scenes," in *European Conference on Computer Vision*, 2016, pp. 549–565.